ON THE BURNING OF A LOW-VOLATILITY LIQUID FUEL IN A LOW-POROSITY MEDIUM

Max A. E. Kokubun

Laboratório de Combustão e Propulsão - Instituto Nacional de Pesquisas Espaciais,
Rodovia Presidente Dutra, km 40 - 12630-000,
+55 12 3186 9357,
max@lcp.inpe.br

Fernando F. Fachini

Laboratório de Combustão e Propulsão - Instituto Nacional de Pesquisas Espaciais,
Rodovia Presidente Dutra, km 40 - 12630-000,
+55 12 3186 9266,
fachini@lcp.inpe.br

Abstract: *In the present work, the aspects of the burning of a liquid fuel inside a low porosity medium is analyzed analytically. The fuel is considered to be low volatile and subjected to an impinging stream of oxidant. The low volatile liquid fuel vaporizes and the diffusion flame is established in the region in which the mass fluxes are in stoichiometric proportion. The Schvab-Zel'dovich formulation is utilized in the gas-solid region in order to eliminate the strong non-linear Arrhenius term from the conservation equations. Own to the differences on the phases transport properties, the system studied presents physical processes occurring in different length scales. By means of the asymptotic theory, expressions for the three phases of the problem are obtained with the aid of the perturbation theory in each length scale and matched in order to obtain the full solution. The relevant parameters of the problem are exhibited and discussed. The proposed model is useful in the study of the in-situ combustion process, a thermal recovery method for heavy oils.*

Keywords: *in-situ combustion, diffusion flame, porous medium.*

1 Introduction

The study of combustion in porous media is of great interest to the areas of science and engineering. Developments of technologies based on features such as heat recirculation, intense radiation field and complete combustion with low emission of pollutants is vastly found in the literature (Howell *et al.*, 1996; Mujeebu *et al.*, 2009, 2010). The singular characteristics that arises from the process of confined combustion also allows the existence of ultra-lean flames in porous media (Loyd and Weinberg, 1974; Wood and Harris, 2008; Tierney *et al.*, 2010; Pereira *et al.*, 2010) and flame temperatures higher than the adiabatic limit (superadiabatic temperatures (Takeno and Sato, 1979; Hanamura *et al.*, 1993; Zhdanok *et al.*, 1995; Pereira *et al.*, 2009)).

The burning of liquid fuels in porous media is usually considered by analyzing a confined spray combustion, such that the droplets are considered to vaporize before they enter the reaction region (Martynenko *et al.*, 1997; Kayal and Chakravarty, 2005). Jugjai and Pongsai (Jogjai and Pongsai, 2007) performed an experimental study of evaporation and combustion of kerosene in porous media without atomization of the liquid fuel. Their results showed that this kind of combustion system could replace spray combustion with the advantages of compactness and low pollutant emission. Suggestions for practical applications of such system were given. Raju and Tien (Raju and T'ien, 2007) considered the liquid fuel to be immersed in the porous matrix and subjected to an impinging stream of oxidant, but the flame was established outside the porous wick. The authors objective was to study heat and mass transport effects in the porous matrix.

The problem of in-situ combustion utilized as a thermal recovery method for heavy oils (Gottfried, 1968; Branch, 1979; Castanier and Brigham, 2003) also presents the burning of liquid fuel in a porous medium. Its importance is easily assessed, since petroleum still is the most utilized combustible nowadays. Petroleum is a non-renewable energy source, and hence, its exploration must be made as efficient as possible. Analytical, numerical and experimental studies are necessary in order to fully understand the dynamics of this thermal recovery method, and hence, improve it. Some effort has been made in order to study the structure of the propagating combustion front in the well, specially when it comes to conditions to sustain the stable flame (Akkutlu and Yortsos, 2003). The usual approach of analysis is to consider the

large scale well dimension processes, because the flame front inside the reservoir has the well dimension (Castanier and Brigham, 2003). However, like free flames, this confined combustion is also controlled by small-scale (porous dimension, gas heat transport length scale and solid heat transport length scale) processes. Therefore, the fully understanding of the effects of these processes in the small scales on the in-situ combustion is vital not only to the fundamental knowledge but also to provides correct physical (sub-grid) models to be used in simulations of well conditions by numerical codes.

With that in mind, the present work extends a previous study, in which a low vaporization regime inside a porous medium was analyzed (Kokubun and Fachini, 2012). In that work, the evaporation regime of a low volatile liquid was analyzed. The liquid was subjected to a stream of hot jet gas, that was injected at high temperatures in the porous medium. In the present work, diffusion flame originated from the burning of a low volatile liquid fuel is studied by means of a simplified model. The flame is supplied by an oxidant jet from one side and from the evaporation of the low volatile liquid fuel from the other side. High rates of interphase heat exchange (gas-solid and liquid-solid) and a low porosity medium are assumed. A single-step global reaction is considered. The thermal expansion of the gas is assumed to be very small, such that it can be neglected.

Own to the differences on the transport properties in gas, liquid and solid phases, the problem presents physical phenomena that occurs in different length scales. These length scales are proportional to $\Gamma^{-n/2}$, in which $n = \{0, 1, 2\}$, and $\Gamma \equiv \bar{\lambda}_s/\bar{\lambda}_g >> 1$ is the ratio between the solid and gas thermal conductivities. In order to avoid the strong non-linear Arrhenius term, the Schvab-Zel'dovich formulation is employed (Liñan and Williams, 1993; Fachini, 2007) and the problem in the gas-solid region is determined in terms of the mixture fraction and excess enthalpy variables, by considering unitary Lewis number for the oxidant and for the fuel. By means of an asymptotic method, the conservation equations are solved in each length scale. The interphase heat exchange couples the three phases of the problem.

The assumption of negligible small thermal expansion for the gas, although unrealistic, allows us to obtain analytical solutions that otherwise would not be achievable. Even with such approximation, the proposed analysis is able to accurately model the processes that influence the relevant parameters of the problem (vaporization rate, flame position, solid phase temperature at the gas-liquid interface and flame temperature). Justifications on the relevance of the approximation of constant gas density in combustion problems may be found elsewhere (Matkowsky and Sivashinsky, 1979; Matalon, 2009).

2 Mathematical formulation

The gas flow field of the present study is similar to previous works (**?**) and it is defined by the flow velocity $f(\eta) \equiv -a^{1/2}v$ normal to the liquid surface, in which η is the vertical spatial coordinate in the gas-solid region normalized by the characteristic scale $z_s \equiv \bar{\lambda}_s/(v_\infty c_p \rho_\infty)$. The non-dimensional strain-rate $a \equiv z_s/\bar{v}_\infty \, d\bar{u}/d\bar{x}|_\infty$ is defined in terms of the injection velocity, $\bar{v}_\infty$. The combustion process is analyzed through the normalized mixture fraction and excess enthalpy variables, defined respectively as $Z \equiv S\, y_F - y_O + 1$ and $H \equiv (S+1)\theta_g/q + y_F + y_O$ (the oxidant mass fraction y_O is normalized by its initial value $Y_{O\infty}$), by considering the Lewis number for fuel and oxidant equal one and $S \equiv s/Y_{O\infty}$. Hence, the non-dimensional conservation equations of the problem are given by

$$U = f', \tag{1}$$

$$\Gamma^{-1} Pr f''' + f f'' - (f')^2 - \Gamma \varepsilon \beta Pr f' = -\varepsilon Pr\,(1 + \beta\Gamma)\,, \tag{2}$$

$$\Gamma^{-1} Z'' + f Z' = 0, \tag{3}$$

$$\Gamma^{-1} \varepsilon H'' + \varepsilon f H' + \Gamma n_g (\theta_s - \theta_g)(S+1)/q = 0, \tag{4}$$

$$0 = (1-\varepsilon)\theta_s'' - \Gamma n_g (\theta_s - \theta_g), \tag{5}$$

in which Pr is the Prandtl number, β is a unitary order permeability parameter, the variable U is the modified flow velocity tangent to the liquid surface, θ is the temperature measured by the injection gas temperature, and y_F is the fuel mass fraction and the parameter $q \equiv Q/\,(c_p T_\infty)$ is the non-dimensional heat release from the flame. The permeability of the medium is assumed to be low, such that $\kappa = O(\Gamma^{-2})$, in which $\kappa \equiv aK/z_s^2$ is the non-dimensional and modified permeability. A more detailed discussion on the importance to the flow field of the non-dimensional parameter κ is given in (Kokubun and Fachini, 2011).

The gas velocity at the interface is given by $f(0)$. The other boundary conditions at the interface are given by $f'|_0 = 0$, $Z(0) = S\,y_{FS} + 1$, $H(0) = (S+1)\theta_B/q + y_{FS}$ and $\theta_s(0) = \theta_{s0}$, while for $\eta \to +\infty$ the boundary conditions are given by $f'|_\infty = U_\infty$, $Z(\infty) = 0$, $H(\infty) = (S+1)/q + 1$ and $\theta_s(\infty) = 1$. The subscript B, g, l, s, S and ∞ stand for boiling condition, gas phase, liquid phase, solid phase, surface condition and injection condition, respectively, and $(\,)'$ represents the ordinary derivative in η.

For the liquid-solid region the governing equations are given by

$$\varrho_l v_l = \dot{m}, \tag{6}$$

$$\varepsilon J\theta_l'' - \varepsilon M\theta_l' = -\Gamma^2 n_l(\theta_s - \theta_l), \tag{7}$$

$$(1-\varepsilon)\theta_s'' = \Gamma^2 n_l(\theta_s - \theta_l), \tag{8}$$

in which $M \equiv \dot{m}(c_l/c_p)$ is the modified vaporization rate and $J \equiv \bar{\lambda}_l/\bar{\lambda}_s$ is the ratio between liquid and solid thermal conductivities. The normalized spatial coordinate in the liquid-solid region is z. The boundary conditions are given by $\theta_l(-\infty) = \theta_s(-\infty) = \theta_{-\infty}$. Mass and energy conservation at the interface are given, respectively, by

$$\Gamma^{-1}\, y_F'|_{\eta\to 0^+} = (1 - y_{FS})f(0), \tag{9}$$

$$\Gamma^{-1}\varepsilon\, \theta_g'\big|_{\eta\to 0^+} = -\Gamma\tilde{l}f(0) + \varepsilon a^{-1/2} J\, \theta_l'|_{z=-z_B} - \Gamma^2 a^{-1/2} n_l \int_{-z_B}^{0} (\theta_s - \theta_l)dz, \tag{10}$$

in which $z_B = O(\Gamma^{-1})$ is the thickness of the boiling zone. The gas phase velocity at $\eta = 0^+$ is related with the vaporization rate, $\dot{m}$, and with the non-dimensional strain-rate, a, through

$$-a^{1/2} f(0) = \dot{m}. \tag{11}$$

Details on the formulation are given elsewhere (Kokubun and Fachini, 2011, 2012).

The conservation equations are solved by means of the singular perturbation theory (Van Dyke, 1964; Kevorkian and Cole, 1981). Hence, the solutions are considered to be given by $\Delta = \Delta_{(0)} + \sum_{n=1}^{+\infty} \Gamma^{-n/2}\Delta_{(n/2)}$ in each length scale and imposed to match with the neighboring scales.

In a previous work (Kokubun and Fachini, 2012), in which no flame was considered, it was obtained that $f(0) = \Gamma^{-1}f_1 + \Gamma^{-2}f_2$ (which results in a leading order vaporization rate given by $\dot{m} = O(\Gamma{-}1)$) and that the solid phase temperature at the interface was $\theta_{s0} = \theta_B + \Gamma^{-1}\theta_{s1}$. The existence of the flame in the present analysis enhances the heat transport to the liquid phase (mainly by the solid phase heat conduction), increasing the vaporization rate and the solid phase temperature at the interface. These enhancements are taken into account mathematically by considering in the present work that $f(0) = \Gamma^{-1/2}f_{1/2} + \Gamma^{-3/2}f_{3/2}$ and $\theta_{s0} = \theta_B + \Gamma^{-1/2}\theta_{s1/2}$.

2.1 Gas-solid region

Above the interface, gas flow fills the solid matrix. In an unitary order region from the liquid fuel pool, the flow field is a result of the injected oxidant stream, while in the region very close to the interface, the flow field is a result from the vaporization of the liquid fuel. In the region in which the mass fluxes are in a stoichiometric proportion the flame is established and assumed that its distance from the liquid surface to be of the order of $\Gamma^{-1/2}$. Therefore, this region is denominated as the flame zone and it is of the order of $\Gamma^{-1/2}$. Since the heat transfer between gas and solid is assumed to be high (of the order of Γ), thermal equilibrium is observed in most part of the gas-solid region, even in the flame zone, in which the heat release is intense. Only in the viscous region near the gas-liquid interface thermal non-equilibrium is observed, own to the differences in the transport properties of gas and solid phases. This small zone is denominated as the inner zone, and it is of the order of Γ^{-1}. Since the solid matrix is assumed to be of low porosity, the heat generated in the flame zone is mainly transported by conduction towards the inner zone. At the interface, the gas is in thermal equilibrium with the liquid fuel, at its boiling temperature, while the solid is at a slightly higher temperature. This temperature difference is the main responsible for providing to the liquid fuel the necessary heat to undergo phase change.

2.2 Outer zone: region of the order of unity

In a region of the order of unity away from the gas-liquid interface, solid and gas are in thermal equilibrium due to the high rates of interphase heat exchange, and hence, it is considered $\theta_s = \theta_g = \theta$. The flow field in this zone is dominated by the Darcy equation. The profiles are given by

$$f(\eta) = \eta - \Gamma^{-1}\frac{(1-\varepsilon Pr)}{(\varepsilon\beta Pr)}\eta + O(\Gamma^{-2}), \tag{12}$$

$$H(\eta) = 1 + \frac{(S+1)}{q}\left[\theta_f - (\theta_f - 1)\ \mathrm{erf}\left(\eta/\left(2\gamma\right)^{1/2}\right)\right] + O(\Gamma^{-1}), \tag{13}$$

$$\theta(\eta) = \theta_f - (\theta_f - 1)\ \mathrm{erf}\left(\eta/\left(2\gamma\right)^{1/2}\right) + O(\Gamma^{-1}), \tag{14}$$

in which θ_f is the flame temperature and $\gamma \equiv (1-\varepsilon)/\varepsilon$ is the porosity parameter. In this zone the vaporized fuel is not observed, since its transport is a process restricted to the region close to the interface. Hence, in the outer zone, $Z(\eta) = 0$.

2.3 Flame zone: region of the order of $\Gamma^{-1/2}$

In a region of the order of $\Gamma^{-1/2}$ from the interface, convective and diffusive mass transport balance. In this region, fuel and oxidant are consumed and the flame is established. Even with the existence of the heat release due to the exothermic chemical reaction, thermal equilibrium still exists due to the intense value of the interphase heat exchange. The vaporized fuel is observed in this region, since $f(0) = O(\Gamma^{-1/2})$.

The governing equations in this zone are obtained by stretching the spatial coordinate as $\hat{\eta} = \Gamma^{1/2}\eta$. The solutions for the flame zone are then given by

$$f(\hat{\eta}) = \Gamma^{-1/2}\left(\hat{\eta} + f_{1/2}\right) - \Gamma^{-3/2}\left(\frac{(1-\varepsilon Pr)}{(\varepsilon\beta Pr)}\hat{\eta} - f_{3/2}\right) + O(\Gamma^{-2}), \tag{15}$$

$$Z(\hat{\eta}) = \frac{\mathrm{erfc}\left((\hat{\eta} + f_{1/2})2^{-1/2}\right)}{\mathrm{erfc}\left((\hat{\eta}_f + f_{1/2})2^{-1/2}\right)} + O(\Gamma^{-1}), \tag{16}$$

$$\theta(\hat{\eta}) = \begin{cases} \theta_f - \Gamma^{-1/2}\left(2/\pi\gamma\right)^{1/2}\ (\theta_f - 1)\left(\hat{\eta}_f - \hat{\eta}\right) + O(\Gamma^{-3/2}), & Z < 1 \\ \theta_B + (\theta_f - \theta_B)\ \hat{\eta}/\hat{\eta}_f + \Gamma^{-1/2}\theta_{s1/2} + \Gamma^{-1}(\theta_f - \theta_B)\times \\ \left[(\hat{\eta}^3 - \hat{\eta}_f^2\hat{\eta})/\left(6\gamma\hat{\eta}_f\right) + \left(\hat{\eta}_f/3 + f_{1/2}\right)/\left(2\gamma\right)\hat{\eta}\right] + O(\Gamma^{-3/2}), & Z > 1. \end{cases} \tag{17}$$

$$H(\hat{\eta}) = \begin{cases} 1 + (S+1)\theta_f/q - \mathrm{erfc}\left((\hat{\eta} + f_{1/2})2^{-1/2}\right)/\mathrm{erfc}\left((\hat{\eta}_f + f_{1/2})2^{-1/2}\right) + O(\Gamma^{-1}), & Z < 1 \\ (S+1)\theta_f/q + \Big[(2/\pi)^{1/2}\ e^{-\left(\hat{\eta}_f + f_{1/2}\right)^2/2}(S+1)\left(\hat{\eta} - \hat{\eta}_f\right) - \\ \mathrm{erf}\left((\hat{\eta} + f_{1/2})2^{-1/2}\right) + \mathrm{erf}\left((\hat{\eta}_f + f_{1/2})2^{-1/2}\right)\Big]/\left(S\ \mathrm{erfc}\left((\hat{\eta}_f + f_{1/2})2^{-1/2}\right)\right) + O(\Gamma^{-1}), & Z > 1, \end{cases} \tag{18}$$

in which $\hat{\eta}_f$ is the normalized flame position and $f_{1/2}$ is the leading order gas-phase velocity at the interface.

2.4 Inner zone: region of the order of Γ^{-1}

In the length scale of the order of $\Gamma^{-1} << 1$ from the interface, thermal non-equilibrium between phases prevails. However, such non-equilibrium is only observed in higher orders, due to the low values of the flow velocity. Only the vaporized fuel, that is transported by diffusion, is observed in this region.

Stretching the spatial variable as $\tilde{\eta} = \Gamma^{1/2}\hat{\eta}$ and solving the conservation equations, the following profiles are obtained for the inner, viscous zone

$$f(\tilde{\eta}) = \Gamma^{-1/2}f_{1/2} + \Gamma^{-1}\left[\tilde{\eta} - (\varepsilon\beta)^{-1/2}\left(1 - e^{-(\varepsilon\beta)^{1/2}\tilde{\eta}}\right)\right] + \Gamma^{-3/2}\left\{f_{3/2} + \right.$$

$$\left. f_{1/2}\left(2Pr\left(\varepsilon\beta\right)^{1/2}\right)^{-1}\left[\tilde{\eta}\ e^{-(\varepsilon\beta)^{1/2}\tilde{\eta}} + (\varepsilon\beta)^{-1/2}\left(e^{-(\varepsilon\beta)^{1/2}\tilde{\eta}} - 1\right)\right]\right\} + O(\Gamma^{-2}) \tag{19}$$

$$Z(\tilde{\eta}) = S\, y_{FS} + 1 + \Gamma^{-1/2} \frac{2^{1/2}\ e^{-f_{1/2}^2/2}}{\pi^{1/2}\mathrm{erfc}\left(2^{-1/2}(\hat{\eta}_f + f_{1/2})\right)}\, \tilde{\eta} + O(\Gamma^{-1}), \tag{20}$$

$$H(\tilde{\eta}) = (S+1)\theta_B/q + y_{FS} + \Gamma^{-1/2} \left\{ 2^{1/2} \frac{(S+1)e^{-(\hat{\eta}_f + f_{1/2})^2/2} - e^{-f_{1/2}^2/2}}{\pi^{1/2} S\ \mathrm{erfc}\left((\hat{\eta}_f + f_{1/2})2^{-1/2}\right)} \tilde{\eta} + \right.$$
$$\left. (S+1)\theta_{s1/2}\left(1 - e^{-(n_g/\varepsilon)^{1/2}\tilde{\eta}}\right)/q \right\} + O(\Gamma^{-1}), \tag{21}$$

$$\theta_s(\tilde{\eta}) = \theta_B + \Gamma^{-1/2}\left[\theta_{s1/2} + (\theta_f - \theta_B)\hat{\eta}_f^{-1}\tilde{\eta}\right] + \Gamma^{-3/2}\gamma^{-1}\left[\theta_{s1/2}\left(e^{-(n_g/\varepsilon)^{1/2}\tilde{\eta}} - 1\right) - \right.$$
$$\left. (\theta_f - \theta_B)\left(\hat{\eta}_f/3 + f_{1/2}\right)\tilde{\eta}/2\right] + O(\Gamma^{-2}), \tag{22}$$

$$\theta_g(\tilde{\eta}) = \theta_B + \Gamma^{-1/2}\left[\theta_{s1/2}\left(1 - e^{-(n_g/\varepsilon)^{1/2}\tilde{\eta}}\right) + (\theta_f - \theta_B)\hat{\eta}_f^{-1}\tilde{\eta}\right] +$$
$$\Gamma^{-3/2}\left[\theta_{s1/2}\left(1 - e^{-(n_g/\varepsilon)^{1/2}\tilde{\eta}}\right) + (\theta_f - \theta_B)\hat{\eta}_f^{-1}\tilde{\eta}\right] + O(\Gamma^{-2}), \tag{23}$$

in which $f_{3/2}$ is the higher order value of the gas-phase velocity at the interface and $\theta_{s1/2}$ is the correction of the solid phase temperature at the interface.

3 Liquid-solid region

Below the interface, the solid matrix is filled with the liquid fuel. The large contact area between solid and liquid is the main responsible for providing the heat generated in the flame zone to the liquid fuel. The liquid fuel in the reservoir is heated until it reaches its boiling temperature, and in a small region below the interface, all the heat provided to the liquid phase goes to phase change. The intense interphase heat exchange is responsible for bringing thermal equilibrium in most part of the liquid-solid region. Thermal non-equilibrium is only observed in the boiling zone, near the interface.

3.1 Equilibrium zone

In most part of the liquid-solid region, thermal equilibrium is observed. Hence, considering $\theta_s = \theta_l = \theta$, Eqs. (7) and (8) are summed and solved, providing the following solution for the temperature

$$\theta(z) = \theta_{-\infty} + (\theta_B - \theta_{-\infty})\ e^{z\ M/(J+\gamma)}. \tag{24}$$

Since $M \sim f(0) = O(\Gamma^{-1/2})$ (as seen from Eq. (11) and from the definition of M), the exponential term presents a variation of the order of unity in a region of the order of $\Gamma^{1/2}$. In order to obtain the temperature profile for the equilibrium region of the order of unity, Eq. (24) is expanded for small values of z, giving

$$\theta(z) = \theta_B + \frac{(\theta_B - \theta_{-\infty})}{J+\gamma}\left\{\Gamma^{-1/2}M_{1/2}\ z + \Gamma^{-1}\frac{M_{1/2}^2}{2(J+\gamma)}\ z^2 + \Gamma^{-3/2}M_{3/2}\ z + O(\Gamma^{-2})\right\} \tag{25}$$

in which $M = \Gamma^{-1/2}M_{1/2} + \Gamma^{-3/2}M_{3/2}$, and $M_{1/2} \equiv -a^{-1/2}\,(c_l/c_p)\ \ f_{1/2}$, $M_{3/2} \equiv -a^{-1/2}\,(c_l/c_p)\ \ f_{3/2}$.

3.2 Boiling zone: region of the order of Γ^{-1}

When the liquid reaches its boiling temperature, all the heat provided to it goes to phase change. The solid, on the other hand, does not have such constraint and its temperature continues to increase. Hence, thermal non-equilibrium is observed in the boiling zone. This non-equilibrium is the main responsible for providing the necessary heat to the liquid fuel undergo phase change. However, due to the intense heat transfer, this thermal non-equilibrium is only observed in higher orders.

Stretching the spatial variable as $\tilde{z} = \Gamma z$ and solving the conservation equations in the boiling zone, the following temperature profiles are found

$$\theta_l(\tilde{z}) = \theta_B + \Gamma^{-3/2}M_{1/2}(\theta_B - \theta_{-\infty})\,(J+\gamma)^{-1}\,\tilde{z} + O(\Gamma^{-2}), \tag{26}$$

$$\theta_s(\tilde{z}) = \theta_B + \Gamma^{-1/2}\theta_{s1/2}\ e^{(n_l/(1-\varepsilon))^{1/2}\tilde{z}} + \Gamma^{-3/2}M_{1/2}\frac{(\theta_B - \theta_{-\infty})}{J+\gamma}\tilde{z} + O(\Gamma^{-2}), \tag{27}$$

in which it is possible to observe that in the boiling zone $(\theta_s - \theta_l) = O(\Gamma^{-1/2})$.

4 Results and discussion

The flame temperature and the solid phase temperature at the interface are obtained by imposing the continuity of the solid phase heat flux at the interface, while the vaporization rate is obtained from the energy conservation at the interface, given by Eq. (10), and from Eq. (11). Evaluating these equations, it is obtained that

$$\theta_f = \theta_B - \frac{2\gamma}{\hat{\eta}_f/3 + f_{1/2}} \left[(n_g/\varepsilon)^{1/2} \frac{\theta_{s1/2}}{\gamma} - a^{1/2} (c_l/c_p) \frac{(\theta_B - \theta_{-\infty})}{J+\gamma} f_{1/2} \right], \tag{28}$$

$$\theta_{s0} = \theta_0 + \Gamma^{-1/2} (\theta_f - \theta_B) (1-\varepsilon)^{1/2} n_l^{-1/2} \hat{\eta}_f^{-1} + O(\Gamma^{-1}), \tag{29}$$

$$\dot{m} = \Gamma^{-1/2} a^{1/2} (c_l/c_p) \tilde{l}^{-1} \left\{ \theta_{s1/2} (1-\varepsilon)^{1/2} (n_l/a)^{1/2} + \right.$$

$$\left. \Gamma^{-1} \left[\varepsilon (c_l/c_p) J (J+\gamma)^{-1} (\theta_B - \theta_{-\infty}) f_{1/2} + (\varepsilon n_g)^{1/2} \theta_{s1/2} + \varepsilon (\theta_f - \theta_B)/\hat{\eta}_f \right] \right\}. \tag{30}$$

These parameters were obtained in terms of the fuel mass fraction at the interface, y_{FS} and the normalized flame position, $\hat{\eta}_f$.

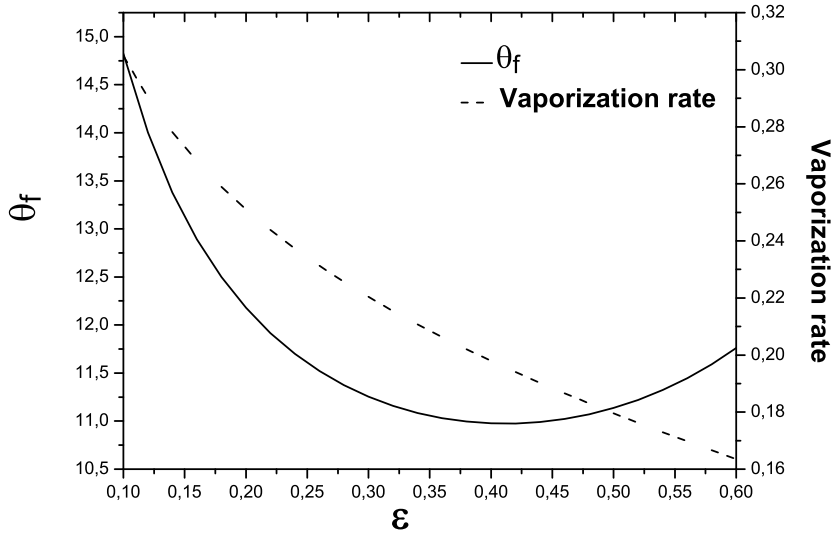

Figure 1: $a = 0.4$

It is possible to observe from Eq. (29) that an increase in the flame temperature leads to an increase in the solid phase temperature at the interface, as one would expect since the heat is mainly transported by conduction through the solid phase. The same effect is observed if the flame gets closer to the interface (decrease in $\hat{\eta}_f$).

Equation (30) points that in its leading order, the vaporization increases as the porosity decreases. Since this process is mainly dominated by the solid-liquid heat exchange in the boiling zone, an increase in the contact area between solid and liquid enhances the vaporization. On the other hand, the gas-liquid heat exchange at the interface is a higher order process (term of the order of $\Gamma^{-3/2}$ in Eq. (30)). This can readily be seen from the fact that an increase in the porosity enhances this higher order process, due to the increase in the contact area between gas and liquid.

The fuel mass fraction at the interface and the flame position are obtained from Eq. (9), expressed for Z, and from Eq. (16) evaluated for $\hat{\eta} \to 0$, giving

$$y_{FS} = 1 + \left(\frac{2}{\pi}\right)^{1/2} \frac{e^{-f_{1/2}^2/2}}{S\ f_{1/2} \mathrm{erfc}\left((\hat{\eta}_f + f_{1/2}) 2^{-1/2}\right)}, \tag{31}$$

$$\mathrm{erf}\left((\hat{\eta}_f + f_{1/2})\, 2^{-1/2}\right) = \frac{\left(\mathrm{erf}\left(f_{1/2} 2^{-1/2}\right) + S\ y_{FS}\right)}{(1 + S\ y_{FS})}. \tag{32}$$

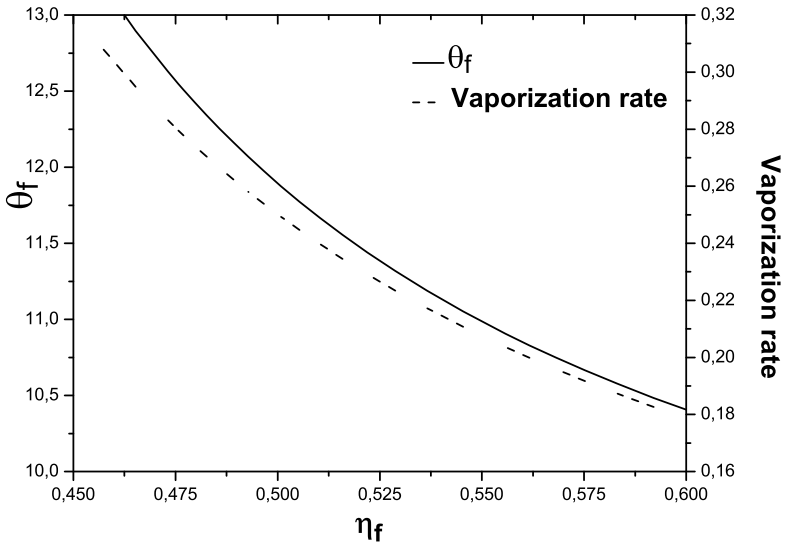

Figure 2: $\varepsilon = 0.3$

Equations (28) to (32) determine the relevant parameters of the problem. This system of equations is highly non-linear, and hence, bifurcations on the solutions may appear. An analysis of a mapping of the parameters space may provide insights over the existence of unstable solutions for the flame, determining the range of existence for this flame.

The following properties were considered $\{\varepsilon, J, n_l, a, n_g\} = \{0.3, 1.0, 1.0, 0.4, 1.0\}$, $\left\{\tilde{l}, S, c_l/c_p\right\} = \{1.0, 15.0, 2.0\}$ and $\{\theta_B, \theta_{-\infty}\} = \{1.34, 1.1\}$. With these values, the parameters are obtained as

$$\eta_f = \Gamma^{-1/2}\hat{\eta}_f = 0.4814, \quad y_{FS} = 0.9982, \quad \theta_f = 8.7132, \quad \theta_{s0} = 1.5536, \quad \dot{m} = 0.3612. \tag{33}$$

Note that the fuel mass fraction at the interface is high, even with the assumption of a low volatile fuel. This is due to the fact that the flame temperature is very high (for an injection temperature of 298K, the flame temperature is almost 2600K).

In Figures (1) and (2) we present the flame temperature and the vaporization rate as functions of the porosity and flame position, respectively. The properties are given by $\{S, \theta_B, \theta_{-\infty}, n_g, n_l, \tilde{l}, J, c_l/c_p\} = \{13.0, 1.34, 1.1, 1.0, 1.0, 1.0, 1.0, 2.0\}$.

From Fig. (1), one can observe that in the low porosity branch (approximately $\varepsilon < 0.35$, for this case, in which $a = 0.4$), as the porosity increases, the flame temperature decreases. This is a result from the increase in the volume occupied by the gas phase, which causes a decrease in the heat recirculation effect. The flame temperature as a function of the porosity presents a minimum and then increases for higher porosity values. From Eq. (28) it is possible to observe that the flame temperature depends on the denominator $(\hat{\eta}_f/3 + f_{1/2})$. Since $f_{1/2}$ is always negative, the denominator in Eq. (28) may approach zero and perform a strong influence on the behavior of the flame temperature profile. In the high porosity branch, the denominator is close to zero, and hence, small variations in its value induces strong variations in the flame temperature. This sensibility indicates that the model is not valid for the branch of high porosities. Since it is assumed in the formulation that the porosity is low, such that the permeability is also low (non-dimensional permeability $\kappa = O(\Gamma^{-2})$), this result is not unexpected.

5 Conclusion

The fluid-mechanical aspects of the burning of a low volatile liquid fuel subjected to a stream of oxidant in a low porosity medium were analyzed by means of the asymptotic theory and the Schvab-Zel'dovich formulation on the gas-solid region. Own to the differences on the transport properties, the problem presents physical processes occurring in different length scales. The profiles were obtained in each length scale and the matching flux condition between scales was imposed. The parameters were then obtained and discussed.

The system analyzed in the present work is of relevance to problems related with the burning of low-volatile fuels in porous medium, specially the process of in-situ combustion, a thermal recovery process for heavy oils. Since this process is not well understood, efforts in every front (analytical, numerical and experimental) must be made in order to achieve higher insights over the process. The present work proposes a simplified model for the in-situ combustion problem. Even though this model is simple, it was able to capture by analytical means the relevant parameters for the problem and its dependencies on the solid, gas and liquid phases properties.

Acknowledgements

The authors greatly acknowledge the Fundação de Amparo à Pesquisa do Estado de São Paulo (FAPESP), under the Grant 2010/18077-1, and the Conselho Nacional de Desenvolvimento Científico e Tecnológico (CNPq), under the Grant 303046/2010-4, for the financial support for the development of this work.

References

Akkutlu, I. Y. and Yortsos, Y. C., 2003, Combust. Flame, Vol. 134, pp. 229-247.
Branch, M. C., 1979, Prog. Energy Combust. Sci., Vol. 5, pp. 193-206.
Castanier, L. M. and Brigham, W. E., 2003, J. Petroleum Sci. & Eng., Vol. 39, pp. 125-136.
Fachini, F. F., 2007, Intl J. Heat Mass Transfer, Vol. 50, pp. 1038-1045.
Gottfried, B. S., 1968, Combust. Flame, Vol. 12, pp. 5-13.
Hanamura, K., Echigo, R. and Zhdanok, S. A., 1993, Intl J. Heat Mass Transfer, Vol. 36, pp. 3201-3209.
Howell, J. R., Hall, M. J. and Ellzey, J. L., 1996, Prog. Energy Combust. Sci., Vol. 22, pp. 121-145.
Jugjai, S. and Pongsai, C., 2007, Combust. Sci. Tech, Vol. 179, pp. 1823-1840.
Kayal, T. K. and Chakravarty, M., 2005, Intl J. Heat Mass Transfer, Vol. 48, pp. 331-339.
Kevorkian, J. and Cole, J. D., Perturbation Methods in Applied Mathematics, Springer-Verlag, Berlin and New York, 1981, pp. 370-387.
Kokubun, M. A. E. and Fachini, F. F., 2012, J. Fluid Mech., Vol. 698, pp. 185-210.
Kokubun, M. A. E. and Fachini, F. F., 2011, Intl J. Heat Mass Transfer, Vol. 54, pp. 3613-3621.
Liñan, A. and Williams, F. A., Fundamental Aspects of Combustion, Oxford University Press, New York, US, 1993, pp. 111-150.
Lloyd, S. A. and Weinberg, F. J., 1974, Nature, Vol. 251, pp. 47-49.
Martynenko, V. V., Echigo, R. and Yoshida, H. 1997, Intl J. Heat Mass Transfer, Vol. 41, pp. 117-126.
Matalon, M., 2009, Proc. Combust. Inst., Vol. 32, pp. 57-82.
Matkowsky, B. J. and Sivashinsky, G. I., 1979, SIAM J. Appl. Math., Vol. 37, pp. 686-699.
Mujeebu, M. A., Abdullah, M. Z. and Abu Bakar, M.Z., 2009, Applied Energy, Vol. 86, pp. 1365-1375.
Mujeebu, M. A., Abdullah, M. Z., Mohamad, A.A., and Abu Bakar, M. Z., 2010, Prog. Energy Combust. Sci., Vol. 36, pp. 627-650.
Pereira, F. M., Oliveira, A. A. M. and Fachini, F. F., 2009, Combust. Flame, Vol. 156, pp. 152-165.
Pereira, F. M., Oliveira, A. A. M. and Fachini, F. F., 2010, J. Fluid Mech., Vol. 657, pp. 285-307.
Raju, M. P. and T'ien, J. S., 2007, J. of Porous Media, Vol. 10, No. 4, pp. 327-342.
Takeno, T. and Sato, K., 1979, Combust. Sci. Tech., Vol. 20, pp. 73-84.
Tierney, C., Wood, S., Harris, A. T. and Fletcher, D. F., 2010, Prog. Comput. Fluid Dyn., Vol. 10, pp. 352-365.
Van Dyke, M., Perturbation Methods in Fluid Mechanics, Academic Press, California, US, 1964, pp. 77-97.
Wood, S. and Harris, A. T., 2008, Prog. Energy Combust. Sci., Vol. 34, pp. 667-684.
Zhdanok, S., Kennedy, L. A. and Koester, G., 1995, Combust. Flame, Vol. 100, pp. 221-231.